H-*ras* deletion protects against angiotensin II–induced arterial hypertension and cardiac remodeling through protein kinase G-Iβ pathway activation

Paloma Martín-Sánchez,[*,†,‡] Alicia Luengo,[*,†,‡] Mercedes Griera,[*,†,‡] María Jesús Orea,[*] Marina López-Olañeta,[§] Antonio Chiloeches,[*] Enrique Lara-Pezzi,[§] Sergio de Frutos,[*,†,‡] Manuel Rodríguez–Puyol,[*,†,‡] Laura Calleros,[*,†,‡,1,2] and Diego Rodríguez–Puyol[†,‡,¶,‖,1]

*Department of Systems Biology and ¶Department of Medicine, Universidad de Alcalá, Madrid, Spain; †Instituto Reina Sofía de Investigación en Nefrológica (IRSIN), Madrid, Spain; ‡Red de Investigación Renal (REDinREN), Instituto de Salud Carlos III, Madrid, Spain; §Myocardial Pathophysiology Area, Centro Nacional de Investigaciones Cardiovasculares, Madrid, Spain; and ‖Nephrology Section, Research Unit Foundation, Hospital Universitario Príncipe de Asturias, Alcalá de Henares, Madrid, Spain

ABSTRACT: Ras proteins regulate cell survival, growth, differentiation, blood pressure, and fibrosis in some organs. We have demonstrated that H-*ras* gene deletion produces mice hypotension *via* a soluble guanylate cyclase-protein kinase G (PKG)–dependent mechanism. In this study, we analyzed the consequences of H-*ras* deletion on cardiac remodeling induced by continuous angiotensin II (AngII) infusion and the molecular mechanisms implied. Left ventricular posterior wall thickness and mass and cardiomyocyte cross-sectional area were similar between AngII-treated H-Ras knockout (H-*ras*$^{-/-}$) and control wild-type (H-*ras*$^{+/+}$) mice, as were extracellular matrix protein expression. Increased cardiac PKG-Iβ protein expression in H-*ras*$^{-/-}$ mice suggests the involvement of this protein in heart protection. *Ex vivo* experiments on cardiac explants could support this mechanism, as PKG blockade blunted protection against AngII-induced cardiac hypertrophy and fibrosis markers in H-*ras*$^{-/-}$ mice. Genetic modulation studies in cardiomyocytes and cardiac and embryonic fibroblasts revealed that the lack of H-Ras down-regulates the B-RAF/MEK/ERK pathway, which induces the glycogen synthase kinase-3β-dependent activation of the transcription factor, cAMP response element-binding protein, which is responsible for PKG-Iβ overexpression in H-*ras*$^{-/-}$ mouse embryonic fibroblasts. This study demonstrates that H-*ras* deletion protects against AngII-induced cardiac remodeling, possibly *via* a mechanism in which PKG-Iβ overexpression could play a partial role, and points to H-Ras and/or downstream proteins as potential therapeutic targets in cardiovascular disease.—Martín-Sánchez, P., Luengo, A., Griera, M., Orea, M. J., López-Olañeta, M., Chiloeches, A., Lara-Pezzi, E., de Frutos, S., Rodríguez-Puyol, M., Calleros, L., Rodríguez-Puyol, D. H-*ras* deletion protects against angiotensin II–induced arterial hypertension and cardiac remodeling through protein kinase G-Iβ pathway activation. FASEB J. 32, 920–934 (2018). www.fasebj.org

KEY WORDS: PKG · CREB · H-*ras*$^{-/-}$ · cardiac hypertrophy

Ras proteins, which belong to the superfamily of small monomeric proteins with GTPase activity, act as molecular switches between inactive and active GDP-bound

cycles. Effects on cell function are exerted by activating several intracellular signaling pathways, mainly *via* activation of RAF effectors and ERK/MAPK and PKB/AKT routes (1, 2). These proteins are highly conserved and control many cellular functions (3–5). Three *ras* genes are expressed in mammals and encode 4 homologous 21-kDa proteins: H-Ras, N-Ras, K-Ras4A, and K-Ras4B (3, 6), each with different functions (7); however, because of their ubiquitous expression, it is difficult to determine the functional specificity of each *ras* gene product. In transgenic mouse models, K-*ras* knockout (KO) embryos die *in utero* (8, 9), but H-*ras*, N-*ras*, K-*ras4A*, or both H- and N-*ras* KO animals are fully viable without apparent phenotypic changes (8, 10, 11).

Although the roles of Ras proteins have been studied in multiple conditions, their involvement in blood pressure regulation and hypertension-induced cardiovascular

remodeling has received less attention. Previous reports have suggested Ras protein involvement in the cellular response to angiotensin II (AngII) (12–14), the major bioactive peptide of the renin-angiotensin system that has been implicated in the pathogenesis of various cardiovascular diseases (15, 16). Our group has analyzed the relationships between H-Ras and blood pressure, demonstrating that H-Ras KO exhibits a reduction in basal blood pressure that is dependent on the increased activation of the vasodilator soluble guanylate cyclase protein kinase G (PKG) pathway (17). Conversely, H-Ras overexpression induces hypertension in experimental animals (18, 19); however, the precise mechanisms that explain the relationships between H-Ras and the above-mentioned proteins that are involved in the regulation of vascular tone have not been adequately defined. No analysis has been conducted to determine whether blocking H-Ras could prevent the cardiovascular remodeling that has been associated with processes characterized by chronic excessive vasoconstriction or insufficient vasodilatation, such as systemic arterial hypertension.

In the present study, we developed a chronic arterial hypertension and cardiac remodeling model induced by continuous AngII infusion in wild-type (H-$ras^{+/+}$) and H-ras KO (H-$ras^{-/-}$) animals. Our results clearly demonstrate the protective effect of H-ras deletion against AngII-induced hypertension and cardiac remodeling, and also that this protection, at least in part, depends on the intracellular increase of PKG-Iβ expression. In addition, experiments using mouse embryonic fibroblasts (MEFs) point to the mechanism that links H-Ras deletion with PKG-Iβ overexpression.

MATERIALS AND METHODS

Drugs and other reagents

AngII, 8-bromo-cGMP (8-Br-cGMP), Sirius red stain, leupeptin, pepstatin A, aprotinin, PMSF, ammonium persulfate, Triton X-100, formaldehyde, guanidinium thiocyanate, formamide, anti–β-actin and anti–glyceraldehyde 3-phosphate dehydrogenase (GAPDH) Abs, Claycomb medium, type I fibronectin, collagenase, and gelatin were purchased from Sigma-Aldrich (St. Louis, MO, USA). Peroxidase-conjugated goat anti-rabbit and anti-mouse IgG were obtained from Chemicon (Temecula, CA, USA). Periodic acid-Schiff stain was obtained from Casa Alvarez (Madrid, Spain). Acrylamide-bisacrylamide was purchased from Merck (Darmstadt, Germany). DMEM, fetal bovine serum, trypsin-EDTA (0.02%), L-glutamine, amphotericin, and penicillin-streptomycin were purchased from BioWhittaker (Walkersville, MD, USA). Culture plates came from Nunc (Kastrup, Denmark). X-Omat films were obtained from Eastman Kodak (Rochester, NY, USA). The ECL chemiluminescence system was obtained from Amersham Pharmacia Biotech (Amersham, United Kingdom). Electrophoresis equipment and the protein MW standard were from Bio-Rad (Hercules, CA, USA). PVDF membrane came from PerkinElmer (Boston, MA, USA). All reagents used were of the highest commercially available grade.

Animals

H-$ras^{-/-}$ were obtained as previously reported (10). A breeding colony of adult H-$ras^{-/-}$ animals has been maintained in our laboratory for more than 10 yr. Animals appeared healthy, the growth and reproductive rates of these mice were indistinguishable from those of wild-type animals, and mutant mice reproduced normally (10). Routine genotyping of DNA that was isolated from mouse tail biopsies was performed by PCR using previously reported primers (10). Animals were housed in a pathogen-free and temperature- and humidity-controlled animal facility with 12-h light/dark periods. Food and water were available *ad libitum*. Male H-$ras^{+/+}$ and H-$ras^{-/-}$ 129svj mice were bred as littermate controls and fed a normal laboratory diet throughout the experiments. Our research was conducted in accordance with the *Guide for the Care and Use of Laboratory Animals* [National Institutes of Health (NIH), Bethesda, MD, USA], and the study was approved by the Animal Care and Use Committee at the University of Alcalá (2011/004).

Primary cultured cells and cell lines

The HL-1 mouse cardiac muscle cell line (Sigma-Aldrich) was maintained in Claycomb culture medium that was supplemented with 10% fetal bovine serum and 20 mM L-glutamine and plated in type I fibronectin-coated dishes (1 μg/cm^2) plus 0.1% gelatin.

Mouse ventricular fibroblasts were isolated (20) from adult mice hearts that were excised and placed in ice-cold Ca^{2+}- and Mg^{2+}-free HBSS. Ventricles were minced into 1-mm^3 pieces and digested with 50 μg/ml trypsin overnight, then digested after with 750 U collagenase in Leibovitz L-15 serum-free medium (Sigma-Aldrich). Cells were dislodged, washed, and filtered through a 0.70-μm cell strainer, then centrifuged and resuspended in DMEM complete medium (4500 mg/L glucose, 10% fetal calf serum) and sequentially preplated 3 times. Adherent fibroblasts were cultured in complete medium. Cells were plated in type I fibronectin-coated dishes. Cardiac fibroblasts were allowed to multiply for 1 wk, split 1:3, cultured for another week, and passaged twice to remove contaminating endothelial cells. MEFs were isolated as previously described (21). Subconfluent cells were serum deprived for 24 h and *in vitro* experiments were performed.

Transient transfections

Subconfluent cells were transfected by using Lipofectamine (Thermo Fisher Scientific, Waltham, MA, USA) for 8 h. To deplete the protein expression of cAMP response element-binding protein (CREB; Santa Cruz Biotechnology, Santa Cruz, CA, USA), H-Ras protein, specific small interfering RNA (siRNA) oligonucleotides, or Silencer as negative control scrambled RNA was used. To perform luciferase assays, human PKG promoter constructs (22)—kindly provided by Dr. M. Lincoln and Dr. H. Sellak (University of South Alabama, Mobile, AL, USA)—and *Renilla* luciferase (internal control) reporter were transfected, and, 24 h later, luciferase activities were measured with FB12 Berthold luminometer using a dual luciferase reporter kit (Promega, Madison, WI, USA). Other constructs transfected were the myc epitope–tagged constitutively active mutant Ras expression plasmid, ^{V12}Ras E37G (pEFm/^{V12}RasG37) (23); constructs for the myc epitope wild-type B-RAF (pEFm/B-RAF), wild-type C-RAF (pEFm/C-RAF), and the kinase-defective C-RAF (pEFm/C-RAF^{KD}, with Lys-to-Ala at codon 399) (24); expression construct that contained the dominant-negative form of myc-tagged ^{N17}H-Ras (pEFm/^{N17}H-Ras) (25); and the hemagglutinin epitope-tagged constitutively active MEK plasmid, pcDNA3-hemagglutinin-MEK (MEKEE, with Ser-to-Glu and Thr-to-Glu mutations at codons S218D S222D), kindly provided by Dr. R. Marais (24).

Treatments and blood pressure measurement

Mice age 3–4 mo were subcutaneously infused for 28 d with saline vehicle or AngII at a dose of 1000 ng/kg/min using Alzet (Cupertino, CA, USA) osmotic minipumps (model 1004). When animals were anesthetized by inhalation of isoflurane 4%, pumps were implanted s.c. on the back between the shoulder blades and hips through a small incision that was closed with surgical glue. All incision sites healed rapidly without the need for any medication. Blood pressure was measured in conscious mice that were placed on a heated platform (Hatteras Instruments, Cary, NC, USA) using a tail-cuff sphygmomanometer (LE 5001 Pressure Meter; Letica Scientific Instruments, Hospitalet, Spain). Data were recorded before and after AngII treatment. Blood pressure was considered as the mean of at least 20 consecutive valid measurements. All mice were trained with the tail-cuff system (17).

Echocardiography and cardiac sampling

Echocardiography was performed under isoflurane anesthesia. Wall thickness was analyzed by transthoracic echocardiography by using a Vevo 2100 system and a 45-MHz probe (VisualSonics, Toronto, ON, Canada). Measurements were taken by a blinded operator with mice placed on a heating pad under light isoflurane anesthesia adjusted to obtain a target heart rate of 500 ± 50 bpm. Two-dimensional and M-mode echocardiography images were recorded in a long and short view at the level of the papillary muscles. Left ventricular posterior wall thickness and left ventricular mass corrected for heart weight were measured from 2-dimensional parasternal long axis images (26). The LV ejection fraction {LVEF = [left ventricular end-diastolic dimension $(LVDD)^3$ − left ventricular end-systolic dimension $(LVSD)^3] \times 100\%$} and fractional shortening {FS = [(LVDD−LVSD)/LVDD] × 100%} were calculated. At the end of the experiment, mice were euthanized by cervical dislocation under anesthesia with inhaled isoflurane 4%. Hearts were excised. Part of this tissue was snap-frozen in RNAlater solution for mRNA and protein experiments, whereas another part was fixed and paraffin embedded for histologic experiments.

Western blot analysis

Tissues or cells were lysed in 50 mM Trizma (pH 8), 150 mM NaCl, 0.1% Triton X-100, 10 mM EDTA, 0.25% sodium deoxycholate, and protease inhibitors. Protein samples were run on SDS-PAGE gels and transferred to PVDF membranes (17). After blocking, immunodetection was performed with the following Abs: anti–PKG-Iβ (Stressgene, ADI-KAP-PK002, RRID:AB_2039484; Enzo Life Sciences, Victoria, BC, Canada) (27); PKG-Iα, p-ERK, ERK, p–glycogen synthase kinase-3β(Ser9) [GSK-3β(Ser9)], GSK-3β, p-CREB(Ser129), p-CREB (Ser133), and CREB (Cell Signaling Technology, Danvers, MA, USA); phosphorylated (p) vasodilator-stimulated phosphoprotein(Ser239) [p-VASP (Ser239)] and VASP (Calbiochem, La Jolla, CA, USA); and TGF-β1, fibronectin, and collagen type I (Abcam, Cambridge, United Kingdom), followed by horseradish peroxidase–conjugated secondary antibodies. Ab-bound proteins were visualized by ECL (Amersham Pharmacia Biotech). Densitometry analyses were performed by using ImageJ software (NIH).

Quantitative RT-PCR analysis

Total RNA was extracted by using Trizol (Thermo Fisher Scientific), and cDNA was prepared by using a Reverse Transcription Kit (Applied Biosystems, Foster City, CA, USA). Quantitative RT-PCR

was performed by using SYBR Green Master Mix (Thermo Fisher Scientific). Primers, designed by using the PubMed Gene Database (National Center for Biotechnology Information, Bethesda, MD, USA; *https://www.ncbi.nlm.nih.gov/pubmed/*), were as follows: (mouse TGF-β1) forward: 5′-TTGCTTCAGCT-CCACAGAGA-3′, reverse: 5′-TGGTTGTAGAGGGCAA-GGAC-3′; (mouse fibronectin) forward: 5′-TGAGCGCCC-TAAAGATTCCA-3′, reverse: 5′-TAGCCACCAGTCTCATGT-GC-3′; (mouse collagen type I) forward: 5′-TCCTGGCAA-CAAAGGAGACA-3′, reverse: 5′-GGGCTCCTGGTTTTC-CTTCT-3′ (mouse PKG-Iα) forward: 5′-AAGCATGATGG-GAAAACAGG-3′, reverse: 5′-GTGACTGCTGGCTTGTGG-TA-3′; (PKG-Iβ) forward: 5′-GACAGCTGCATCATCAAG-GA-3′, reverse: 5′-GATGGCCCAGAGTTTCACAT-3′; (Myh6) forward: 5′-GGTCACCAACAACCCATACG-3′, reverse: 5′-CAGGGTTGCGTTGATGC-3′; (Myh7) forward: 5′-GAAG-GAGGACCAGGTGATG-3′, reverse: 5′-TGACAGTCTTC-CCAGCTCC-3′; and (β-actin) forward: 5′-GACGGCCAGGTC-ATCA-CTAT-3′, reverse: 5′-CTTCTGCATCCTGTCAGCAA-3′. Results are expressed as fold increase by using the $\Delta\Delta C_t$ method normalized to β-actin (26).

Ex vivo experiments

H-*ras*$^{+/+}$ and H-*ras*$^{-/-}$ mice were euthanized by cervical dislocation under anesthesia with inhaled isoflurane 4%. Hearts were extracted and left ventricles were sliced and cultured at 37°C in DMEM-F12 medium that was supplemented with 10% fetal bovine serum, amphotericin, and penicillin-streptomycin under normoxic conditions. Explants were treated for 16 h with 1 μM AngII, with or without PKG inhibitor [100 μM guanosine, 3′,5′-cyclic monophosphorothioate, 8-(4-chlo-rophenylthio)-,Rp-isomer, triethylammonium salt; Calbiochem] or 10 μM 8-Br-cGMP. After treatments, Western blot or quantitative RT-PCR was performed on tissues, as previously described. Tissue integrity was controlled by measuring creatine kinase and lactate dehydrogenase in supernatants.

Histology

Cardiac tissue was fixed in 4% paraformaldehyde and subsequently dehydrated and embedded in paraffin. For Sirius red staining, paraffin heart sections (2–3 μm) were dewaxed, rehydrated, and incubated with Sirius red solution for 60 min; washed in acidified water; dehydrated in ethanol; cleared in xylene; and mounted in a mixture of distyrene, a plasticizer (tricresyl phosphate), and xylene medium (DPX; Sigma-Aldrich). Periodic acid-Schiff staining was performed according to manufacturer protocol. Eight random fields from each heart section were photographed, and the positive areas were calculated by using ImageJ software.

Chromatin immunoprecipitation assay

Standard chromatin immunoprecipitation (ChIP) assays were performed in MEFs as previously described (28). Cells were treated with 1% formaldehyde for 15 min and sonicated to produce chromatin fragments (0.5 kb on average). Predicted CREB-responsive element DNA was immunoprecipitated with an anti-CREB Ab (Cell Signaling Technology). Quantitative PCR reactions were performed by using SYBRGreen PCR Master Mix (Applied Biosystems) and primers that encompassed the PKG-I promoter region [5′-CCGTCTTCAAGTGCAGCAAT-3′ (sense) and 5′-GGATGCTAGCCTGTTACCCA-3′ (antisense)]. Sensitivity of PCR amplification was evaluated on serial dilutions of total DNA that was collected after sonication (input fraction).

Fold enrichment was calculated by using the CREB/isotype control value. A polyclonal Ab against histone H4 was used as positive control.

In silico analysis

In silico analysis was performed using Searching Transcription Factor Binding Sites (TFSearch; Computational Biology Research Center, National Institute of Advanced Industrial Science and Technology, Tokyo, Japan).

Statistical analysis

All data were analyzed by using Prism (v.4.00; GraphPad Software, La Jolla, CA, USA). Results are expressed as means ± SEM. As the number of animals or samples in the different experiments was sometimes <10, nonparametric statistics were used for comparisons, applying the Kruskal-Wallis (nonpaired data) and Friedman (paired data) tests, followed by a Bonferroni multiple-comparison test. A value of $P < 0.05$ was considered to be statistically significant.

RESULTS

Protection of H-*ras*$^{-/-}$ mice against AngII-induced hypertension

As previously described (17), H-*ras*$^{-/-}$ mice had lower systolic, diastolic, and mean arterial pressure than did H-*ras*$^{+/+}$ mice under basal conditions (**Table 1**). Long-term AngII infusion significantly increased arterial blood pressure in both strains of animals, but the increase in mean arterial pressure in H-*ras*$^{+/+}$ mice (30 ± 3 mmHg) was greater than the increase in H-*ras*$^{-/-}$ mice (16 ± 3 mmHg; $P < 0.05$; Table 1). Blood pressure values of AngII-infused H-*ras*$^{-/-}$ animals were comparable to nontreated H-*ras*$^{+/+}$ mice (Table 1). There were no significant differences in heart rate among different experimental groups (Table 1). AngII infusion for 28 d did not modify cardiac and vascular H-Ras levels in H-*ras*$^{+/+}$ animals compared with untreated H-*ras*$^{+/+}$ (Supplemental Fig. 1A, B).

Prevention of AngII-induced abnormal cardiac remodeling and functional changes in H-*ras*$^{-/-}$ mice

AngII infusion induced significant cardiac hypertrophy in wild-type animals as demonstrated by the increased ratio of heart weight to body weight (Table 1). This was consistent with the augmentation of left ventricular posterior wall thickness and left ventricular mass as shown by echocardiography (**Table 2**). Echocardiography also demonstrated the presence of reduced left ventricular ejection fraction and fractional shortening in AngII-treated H-*ras*$^{+/+}$ mice (Table 2), which supports a significant reduction in global cardiac function in treated wild-type animals.

The absence of H-Ras significantly prevented cardiac hypertrophy induced by AngII. The ratio of heart weight to body weight in AngII-treated H-*ras*$^{-/-}$ mice (6.51 ± 0.12 mg/g) was lower than in AngII-treated wild-type mice (7.26 ± 0.24 mg/g; $P < 0.05$; Table 1), although still significantly higher than in control H-*ras*$^{+/+}$ mice (5.58 ± 0.24 mg/g; $P < 0.05$; Table 1). Left ventricular posterior wall length and mass—corrected from heart weight—did not increase after 28 d of AngII treatment in H-*ras*$^{-/-}$ animals compared with AngII-treated wild-type mice. Of interest, there were no differences between the ventricular function parameters of untreated and treated H-*ras*$^{-/-}$ mice (Table 2). Furthermore, there were no differences between the two strains in any of the tested ventricular functions and heart weight parameters under basal, nontreated conditions (Tables 1 and 2).

To analyze the pathologic basis of the increased cardiac size in AngII-treated animals, we measured left ventricle cardiomyocyte size and levels of proliferating cell nuclear antigen expression. AngII significantly increased H-*ras*$^{+/+}$ cardiomyocyte cross-sectional area (**Fig. 1A**), whereas proliferating cell nuclear antigen content remained unchanged (data not shown). This suggests that, at least in part, the genesis of the AngII-induced increase in cardiac size is a result of cardiomyocyte hypertrophy. The AngII-induced increase of cardiomyocyte cross-sectional area was completely prevented by H-*ras* deletion (Fig. 1A).

As changes in heart size may also depend on increased extracellular matrix (ECM) content, we also analyzed this possibility in AngII-treated mice. ECM accumulation at the cardiac interstitial level was assessed by Sirius red staining of the left ventricles (Fig. 1B). Increased Sirius red staining was present in AngII-treated H-*ras*$^{+/+}$ animals, but was almost completely abrogated in AngII-treated H-*ras*$^{-/-}$ mice. Moreover, AngII infusion induced a significant increase in mRNA (**Fig. 2A**) and protein (Fig. 2B) levels of the profibrotic

TABLE 1. *Arterial pressure, heart rates, and heart weights*

Variable	SAP (mmHg)	DAP (mmHg)	MAP (mmHg)	HR (bpm)	HW/BW (mg/g)
Control H-*ras*$^{+/+}$ ($n = 10$)	116.0 ± 2.0	83.7 ± 1.7	93.2 ± 1.7	569 ± 26	5.58 ± 0.24
Control H-*ras*$^{-/-}$ ($n = 12$)	97.8 ± 3.0*	68.1 ± 2.2*	78.4 ± 2.5*	574 ± 17	5.26 ± 0.24
AngII H-*ras*$^{+/+}$ ($n = 9$)	151.1 ± 2.9*,**	108.9 ± 4.2*,**	122.9 ± 3.9*,**	581 ± 22	7.26 ± 0.24*,**
AngII H-*ras*$^{-/-}$ ($n = 10$)	119.4 ± 2.8**,†	82.2 ± 3.2**,†	93.5 ± 4.2**,†	541 ± 26	6.51 ± 0.12*,**,†

H-*ras*$^{+/+}$ and H-*ras*$^{-/-}$ mice were exposed for 28 d to continuous AngII infusion (1000 ng/kg/min) or vehicle (controls). Systolic (SAP), diastolic (DAP), mean (MAP) arterial pressures (mmHg) and heart rate [HR; beats/minute (bpm)] were measured by tail-cuff sphygmomanometer. Heart weight/body weight ratios (HW/BW) were determined after euthanization. Results are expressed as means ± SEM. *$P < 0.05$ *vs.* control H-*ras*$^{+/+}$, **$P < 0.05$ *vs.* control H-*ras*$^{-/-}$, †$P < 0.05$ *vs.* AngII-treated H-*ras*$^{+/+}$.

TABLE 2. *Cardiac structure and function parameters assessed by echocardiography*

| Variable	LVPW (mm)	LVMC (mg)	LVEF (%)	FS (%)
Control H-ras$^{+/+}$ (n = 7)	0.77 ± 0.02	91.5 ± 2.6	69.3 ± 6.7	38.5 ± 5.8
Control H-ras$^{-/-}$ (n = 6)	0.80 ± 0.02	97.3 ± 0.8	63.7 ± 4.9	34 ± 3.5
AngII H-ras$^{+/+}$ (n = 7)	0.93 ± 0.01*,**	122.8 ± 9.1*,**	54.2 ± 8.3*	26.3 ± 6.4*
AngII H-ras$^{-/-}$ (n = 9)	0.84 ± 0.02†	100.5 ± 2.1†	60.8 ± 7	33.4 ± 4.7

H-ras$^{+/+}$ and H-ras$^{-/-}$ mice were exposed for 28 d to continuous AngII infusion (1000 ng/kg/min) or vehicle (controls). Left ventricular posterior wall length (LVPW), left ventricle mass corrected from heart weight (LVMC), left ventricular ejection fraction (LVEF), and fractional shortening (FS) were measured. Results are expressed as means ± SEM. *$P < 0.05$ *vs.* control H-ras$^{+/+}$, **$P < 0.05$ *vs.* control H-ras$^{-/-}$, $^{†}P < 0.05$ *vs.* AngII-treated H-ras$^{+/+}$.

cytokine, TGF-β1, in the left ventricles of AngII-treated H-ras$^{+/+}$ mice. This increase was also completely prevented by H-ras deletion. As expected from Sirius red results, AngII increased the mRNA (Fig. 2C) and protein (Fig. 2D) content of collagen I (COL I) in the left ventricles of H-ras$^{+/+}$ mice—an effect not observed in H-ras$^{-/-}$ animals. Similar findings were observed with fibronectin, another characteristic ECM protein (Supplemental Fig. 2A, B). The basal content of ECM proteins and TGF-β1 did not differ between H-ras$^{+/+}$ and H-ras$^{-/-}$ mice (Figs. 1 and 2 and Supplemental Fig. 2). These results suggest that the absence of H-Ras protects mice against AngII-induced myocardial fibrosis.

Prevention of AngII-induced fibrosis *via* a PKG-Iβ–dependent mechanism in H-ras$^{-/-}$ mice

Figure 3 shows that PKG-Iβ mRNA (Fig. 3A) and protein levels (Fig. 3B) were increased in the left ventricles of H-ras$^{-/-}$ hearts, both in basal and AngII-treated conditions without differences between control and treated H-ras$^{-/-}$ mice. Conversely, no changes in PKG-Iα protein or mRNA levels were observed in the left ventricles of H-ras$^{-/-}$ hearts compared with H-ras$^{+/+}$ littermates, both in basal and AngII-treated conditions (Supplemental Fig. 3A and data not shown). These results suggest that PKG-Iβ,

Figure 1. H-Ras deficiency prevents AngII-induced cardiomyocyte hypertrophy and myocardial fibrosis. H-ras$^{+/+}$ and H-ras$^{-/-}$ mice were exposed to continuous AngII infusion (1000 ng/kg/min) or vehicle (control) for 28 d. A, B) Cardiac left ventricles were stained with periodic acid-Schiff to quantify cardiomyocytes sectional areas (A) and Sirius red to quantify the collagen content (B). Representative pictures and quantification analysis are shown. Scale bars, 50 μm. Values represent means ± SEM (n = 9 control and 11 AngII mice). *$P < 0.05$ *vs.* control H-ras$^{+/+}$, $^{$}P < 0.05$ *vs.* control H-ras$^{-/-}$, $^{#}P < 0.05$ *vs.* AngII-treated H-ras$^{+/+}$.
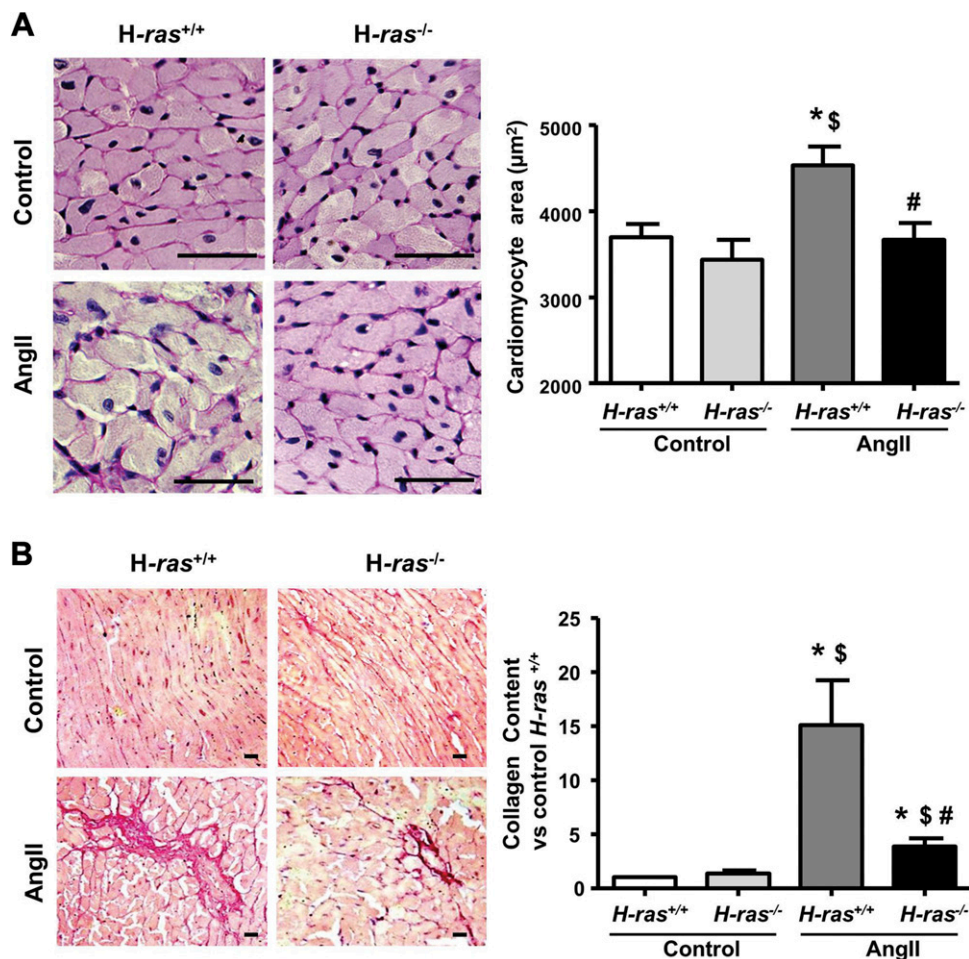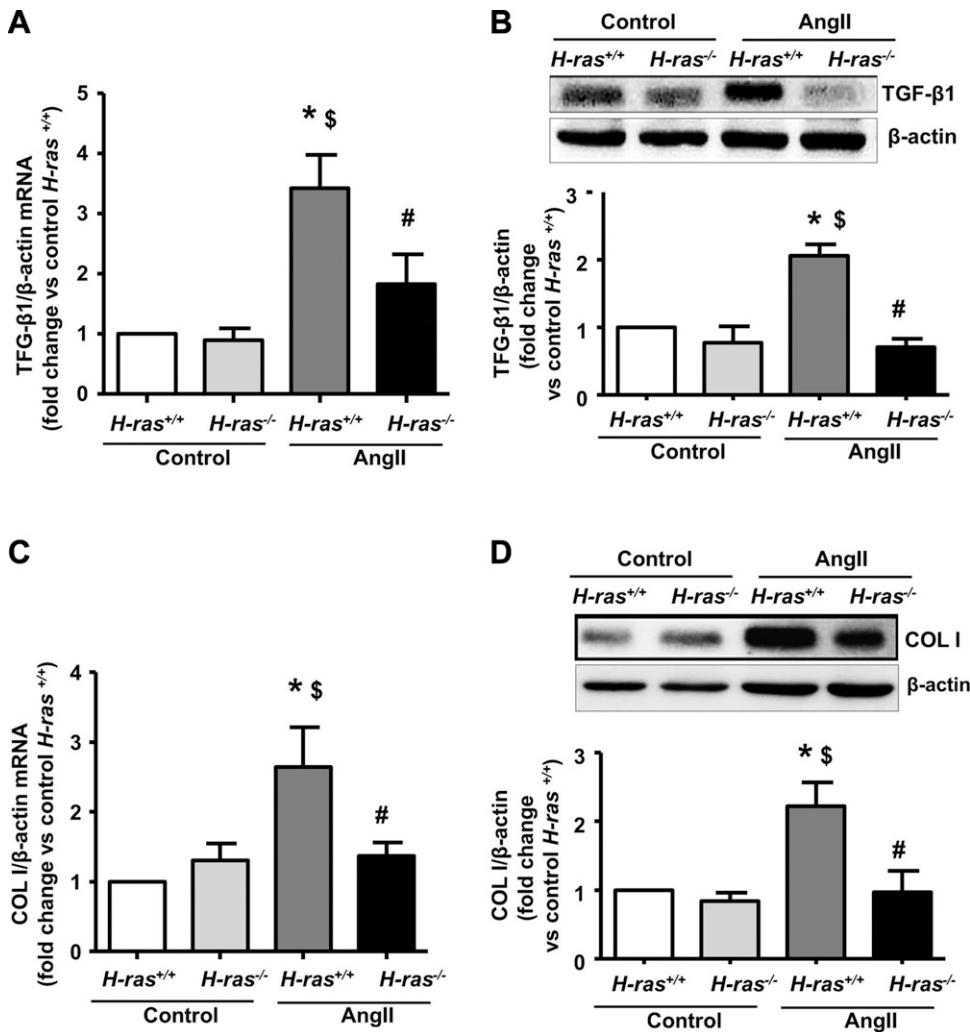
Figure 2. H-Ras deficiency prevents an AngII-induced increase of TGF-β1 and collagen type I expression in cardiac tissue. H-$ras^{+/+}$ and H-$ras^{-/-}$ mice were exposed to continuous AngII infusion (1000 ng/kg/min) or vehicle (control) for 28 d. A, C) Cardiac left ventricles were processed, TGF-β1 (A) and COL I (C) mRNA were normalized against β-actin, and relative fold changes are represented. B, D) Representative immunoblots and densitometric analysis of TGF-β1 (B) and COL I (D) content normalized against β-actin are also shown. Values represent means ± SEM (n = 9 control and 11 AngII). *$P < 0.05$ vs. control H-$ras^{+/+}$, $^{\$}P < 0.05$ vs. control H-$ras^{-/-}$, $^{\#}P < 0.05$ vs. AngII-treated H-$ras^{+/+}$.

but not PKG-Iα, is overexpressed in H-$ras^{-/-}$ mice cardiac tissue.

To analyze the possible role of PKG-Iβ in the prevention of AngII-induced cardiac fibrosis and hypertrophy observed in H-$ras^{-/-}$ mice, we performed *ex vivo* experiments. PKG activity—tested by determining VASP phosphorylation in Ser239—was increased in H-$ras^{-/-}$ heart tissue, both in basal and in 16-h AngII-treated explants, without differences between control and treated H-$ras^{-/-}$ mice (**Fig. 4A**). Moreover, TGF-β1 (Fig. 4B), COL I (Fig. 4C), and fibronectin (Supplemental Fig. 2C) mRNA content increased in H-$ras^{+/+}$-treated explants. These effects were not evident in heart tissue from H-$ras^{-/-}$ mice, which was similar to results obtained in the *in vivo* AngII infusion (Fig. 2 and Supplemental Fig. 2A, B). In addition, analysis of cardiac genes that are associated with the hypertrophy program demonstrated that genes that are normally expressed in the adult heart, such as Myh6, were downregulated (Fig. 4D), whereas expression of fetal genes, such as Myh7 (Fig. 4E), was induced in H-$ras^{+/+}$-treated, but not H-$ras^{-/-}$-treated explants.

Incubation of H-$ras^{+/+}$ heart tissues with the PKG activator, 8-Br-cGMP, increased VASP phosphorylation

(Fig. 4A). It also inhibited the AngII-induced mRNA increases of the profibrotic cytokine, TGF-β1 (Fig. 4B), and ECM proteins, COL I (Fig. 4C) and fibronectin (Supplemental Fig. 2C), and regulated the hypertrophy program marker genes, Myh6 (Fig. 4D) and Myh7 (Fig. 4E). In contrast, a PKG antagonist blunted the increased VASP phosphorylation that was exhibited by heart tissue from H-$ras^{-/-}$ mice (Fig. 4A), which restored the profibrotic and hypertrophic effect of AngII on these hearts (Fig. 4B–E and Supplemental Fig. 2C). Taken together, these results suggest that H-$ras^{-/-}$ mice were protected against AngII-induced heart fibrosis and hypertrophy *via* a mechanism that, at least in part, is PKG-Iβ overexpression dependent.

Mechanisms involved in PKG-Iβ overexpression observed with H-*ras* deletion

To study the mechanisms that are involved in the increased PKG-Iβ expression that was observed in cells that lack H-*ras*—and by extension, in cardiac tissue from H-$ras^{-/-}$ mice—we studied the effects of H-*ras* deletion in a cardiac muscle cell line (HL-1) where H-Ras content was
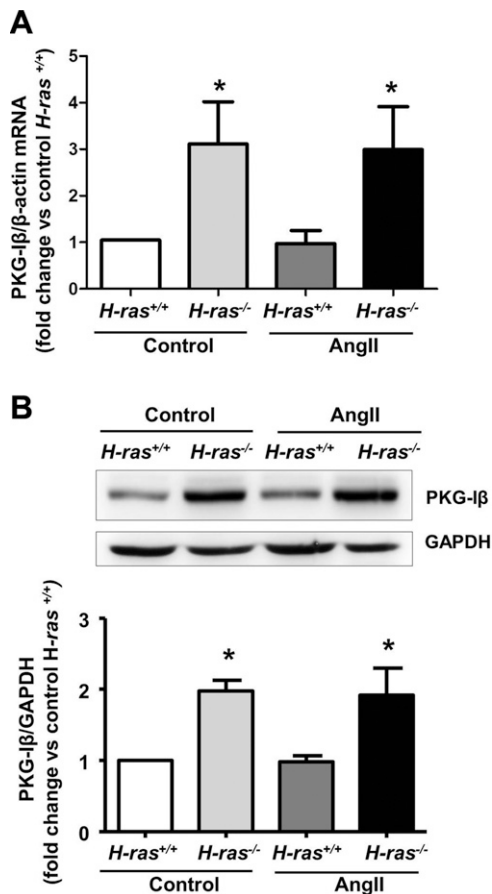
A

B

Figure 3. H-Ras deficiency increases PKG-Iβ mRNA and protein content in cardiac tissue. H-$ras^{+/+}$ and H-$ras^{-/-}$ mice were exposed to continuous AngII infusion (1000 ng/kg/min) or vehicle (control) for 28 d. *A*) Cardiac left ventricles were processed, PKG-Iβ mRNA was normalized against β-actin, and the relative fold changes were represented. *B*) Representative immunoblots and densitometric analysis of PKG-Iβ content normalized against GAPDH are also shown. Values represent means ± SEM ($n = 9$ control and 11 AngII mice). *$P < 0.05$ *vs.* H-$ras^{+/+}$.

abrogated by specific siRNA (Supplemental Fig. 4*A*), and in cultured adult mouse cardiac fibroblasts or MEFs from H-$ras^{+/+}$ and H-$ras^{-/-}$, with a sustained deletion of H-Ras (Supplemental Fig. 4*B, C*). These cell types exhibited the same increased expression of PKG-Iβ (**Fig. 5**) as well as unchanged PKG-Iα levels (Supplemental Fig. 3*B–D*) as intact animals. Moreover, H-*ras* deletion–dependent increased PKG-Iβ expression levels were confirmed by transient transfections of HL-1 cells—with or without H-Ras—or cardiac fibroblasts from both strains, with the complete human PKG-I promoter linked to a luciferase reporter (Supplemental Fig. 5*A, B*). Changes in PKG-Iβ expression were accompanied by increased protein activity, as determined by VASP phosphorylation analysis (Supplemental Fig. 5*C, D*).

For additional analysis, we next transfected MEFs from both strains with constructs that contained serial deletions of the human PKG-I promoter linked to a luciferase reporter. As expected, H-$ras^{-/-}$ MEFs displayed increased luciferase activity of the whole PKG-I promoter region

compared with wild-type MEFs, but the difference disappeared when the fragment between the 2 and 1.5 kb from the promoter sequence was deleted. Subsequent deletions did not induce additional changes in luciferase activity (**Fig. 6***A*). These results suggest that the potential recognition zone for the H-Ras–dependent transcriptional regulation of PKG-Iβ may be located between the first 2 and 1.5 kb from the promotor sequence.

An *in silico* analysis of this region (TFSearch) revealed a putative consensus binding sequence for the transcription factor, CREB. CREB activation was assessed in wild-type and H-$ras^{-/-}$ MEFs by determining its phosphorylation levels in Ser133 and Ser129 (29). We found increased CREB phosphorylation of Ser129 in H-$ras^{-/-}$ MEFs, but not of Ser133 (Fig. 6*B*). Neither serine residue in wild-type MEFs demonstrated increased phosphorylation. To confirm the role of CREB in the increased PKG-I promoter transcriptional activity, we performed quantitative ChIP for CREB-responsive element occupancy at the 5′-regulatory region of the PKG-I promoter. The relative increase of CREB binding to the PKG-I promoter in H-$ras^{-/-}$ MEFs (4.8 ± 1.1) was greater than the relative binding in H-$ras^{+/+}$ MEFs (1.0 ± 0.2; $n = 3$; $P < 0.05$); therefore, we hypothesized that CREB is the transcription factor that is involved in PKG-Iβ up-regulation in the absence of H-*ras*. This hypothesis was strongly supported when the depletion of CREB expression by a specific siRNA abolished increased PKG-I promoter activity (Fig. 6*C*) and PKG-Iβ protein levels (Fig. 6*D*) in H-$ras^{-/-}$ MEFs.

To better understand the signaling pathway between H-Ras depletion and the increased CREB activity implicated in PKG-I promoter transcription, we analyzed the possible role of GSK-3β, one of the upstream kinases that are responsible for CREB phosphorylation of Ser129 (29). H-$ras^{-/-}$ MEFs exhibited a decreased phosphorylation at Ser9 of GSK-3β (**Fig. 7***A*), a post-transductional modification that activates the protein (30), whereas lithium chloride treatment induced increased phosphorylation of GSK-3β in Ser9 (Fig. 7*A*), with the subsequent inhibition of the enzyme (30). The lithium chloride–dependent increased GSK-3β phosphorylation was observed in both types of MEFs, but it was less pronounced in H-$ras^{-/-}$ MEFs (Fig. 7*A*). Treatment of H-$ras^{-/-}$ MEFs with lithium chloride prevented the increased CREB phosphorylation (Fig. 7*B*) and PKG-Iβ overexpression (Fig. 7*C*) that characterized MEFs. These results support the idea that increases in CREB phosphorylation and PKG-Iβ content in H-$ras^{-/-}$ cells are mediated *via* activation of GSK-3β.

Because GSK-3β phosphorylation at Ser9 is mediated by ERK (31), we studied the possible role of the RAF/MEK/ERK canonical Ras-downstream kinase cascade in the regulation of GSK-3β activity. H-$ras^{-/-}$ MEFs have decreased ERK phosphorylation (**Fig. 8***A*)—and thus, decreased activity—compared with wild-type fibroblasts. We verified the pathway implication in cardiac tissues (Supplemental Fig. 6*A*) and in cardiac muscle cell line (Supplemental Fig. 6*B*) and cardiac fibroblasts that were isolated from hearts of adult animals of both genotypes (Supplemental Fig. 6*C*). In addition, transfection with the mutant expression plasmid, ^{V12}RasG37, which selectively
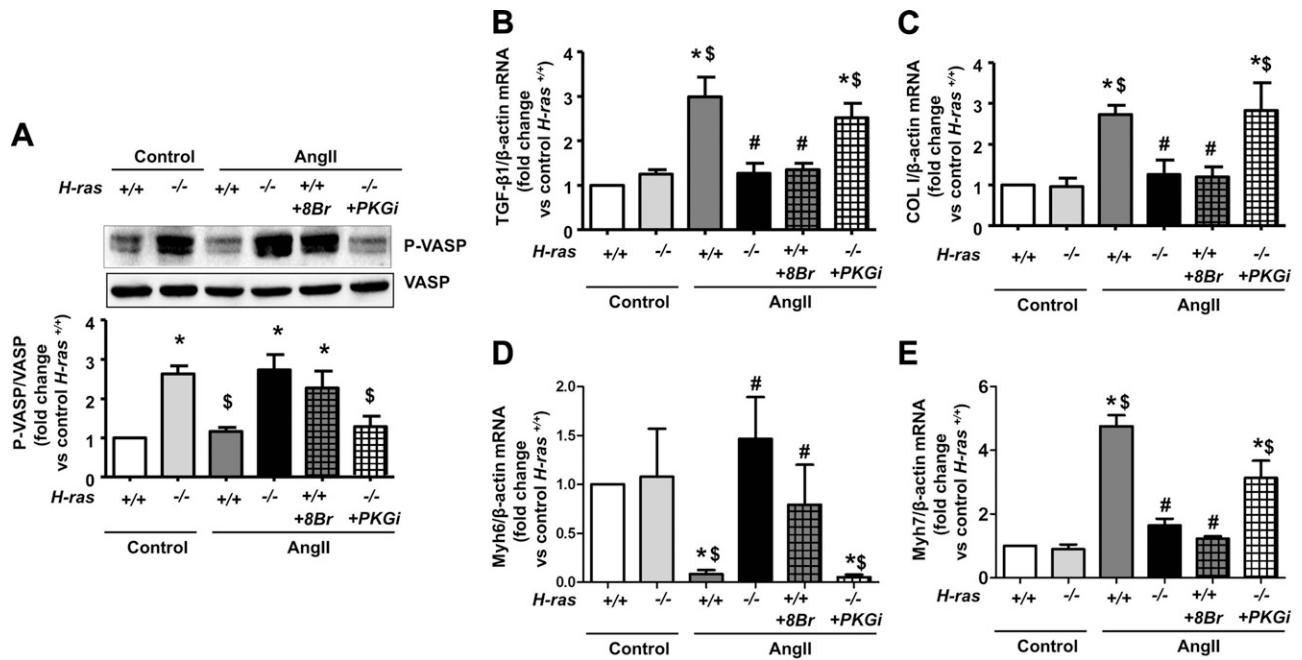
Figure 4. PKG-Iβ is involved in H-Ras–dependent protection against an AngII-induced increase of TGF-β1, COL I, and Myh7, and a decrease of Myh6 expression in cardiac tissue. Cardiac left ventricle explants from H-ras$^{+/+}$ and H-ras$^{-/-}$ mice were exposed *ex vivo* to AngII (1 μM) or vehicle (control) for 16 h, and were cotreated with 8-Br-cGMP (8-Br; 10 μM) or PKG inhibitor (PKGi; 100 μM), respectively. *A*) Representative immunoblots and densitometric analysis of p-VASP content normalized against total VASP are shown. *B–E*) TGF-β1 (*B*), COL I (*C*), Myh6 (*D*), and Myh7 (*E*) mRNA were normalized against β-actin, and relative fold changes are represented. Values represent means ± SEM ($n = 5$). *$P < 0.05$ *vs.* control H-ras$^{+/+}$, $^{\$}P < 0.05$ *vs.* control H-ras$^{-/-}$, $^{\#}P < 0.05$ *vs.* AngII-treated H-ras$^{+/+}$.

activates RAF, or with a constitutively active MEK plasmid, MEKEE, increased ERK (Fig. 8*A*) and GSK-3β phosphorylation (Fig. 8*B*). Transfection also decreased CREB phosphorylation (Fig. 8*C*) and PKG-Iβ protein content (Fig. 8*D*) in H-ras$^{-/-}$ MEFs. In contrast, over-expression of the dominant-negative ^{N17}H-Ras plasmid in H-ras$^{+/+}$ MEFs induced the same ERK, GSK-3β, and CREB phosphorylation states and PKG-Iβ protein content that was present in H-ras$^{-/-}$ MEFs (Supplemental Fig. 7).

To study RAF isoforms that are involved in the H-Ras–dependent modulation of PKG-Iβ, we transiently transfected H-ras$^{-/-}$ MEFs with wild-type B-RAF or C-RAF isoform–overexpressing plasmids. Overexpression of B-RAF, but not C-RAF, in H-ras$^{-/-}$ MEFs restored ERK, GSK-3β, and CREB phosphorylation states and PKG-Iβ protein content to control H-ras$^{+/+}$ values (**Fig. 9**). As expected, kinase-defective C-RAF isoform overexpression did not exert any effect on H-ras$^{+/+}$ MEFs (Supplemental Fig. 7). Taken together, these results indicate that down-regulation of the canonical H-Ras/B-RAF/MEK/ERK signaling pathway *via* activation of GSK-3β and transcription factor CREB were responsible for the PKG-Iβ overexpression that occurs in H-ras$^{-/-}$ cells (**Fig. 10**).

DISCUSSION

There are two main experimental approaches in the present work. A first group of studies performed in animals and cardiac explants demonstrates that H-Ras

deficiency does indeed prevent AngII-induced hypertension and cardiac remodeling and leads us to speculate that this remodeling prevention depends, at least in part, on PKG-Iβ overexpression. A second group of studies performed in cultured cells confirmed the link between H-ras and PKG-Iβ expression and defined the implied mechanism.

The association between AngII and myocardial remodeling has been previously reported. AngII has been identified as a stimulator of rodent cardiomyocyte hypertrophy (32, 33), with minor changes in cardiomyocyte proliferation (34). Left ventricular remodeling is also characterized by interstitial fibrosis. Indeed, one common characteristic that underlies nearly all forms of heart failure is the excessive deposition of ECM, which is often associated with decreased ventricular compliance (15). Reports suggest that, in patients with hypertension and in a mouse model of pressure overload, heart failure and the increased cardiac ECM deposition are related to the activation of the local renin-angiotensin system (35, 36). In this context, angiotensin-converting enzyme inhibitors or AngII receptor blockers are effective in ameliorating heart failure, alleviating ECM deposition, and reducing cardiac remodeling (15). Furthermore, a large body of evidence suggests that the profibrotic cytokine, TGF-β1, promotes the synthesis of ECM components and that the development of cardiac fibrosis is controlled by a regulatory network that involves AngII and TGF-β1 (37, 38). In accordance with these findings, ours results demonstrate that AngII treatment for 28 d induced an
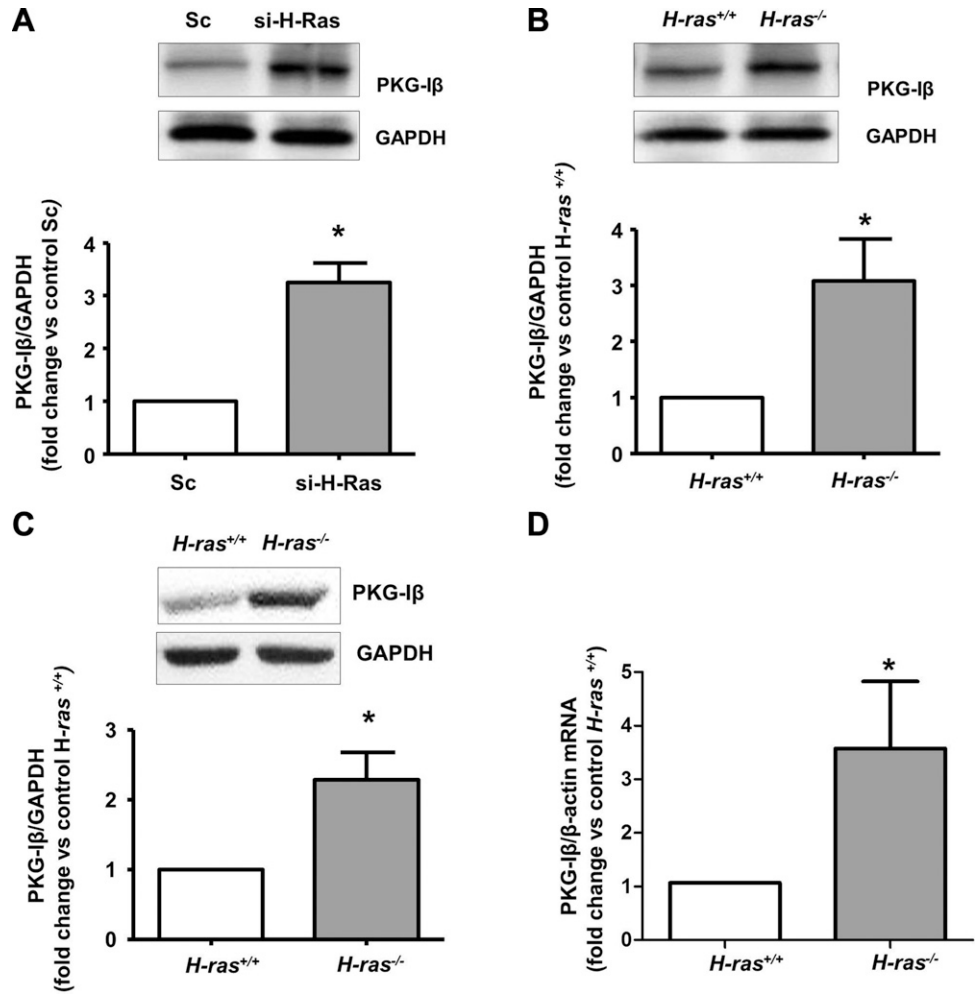
Figure 5. H-Ras deficiency increases PKG-Iβ expression in mouse cardiomyocytes, cardiac fibroblasts, and embryonic fibroblast. *A*) The mouse cardiac muscle cell line (HL-1) was transiently transfected with siRNAs against H-Ras (si-H-Ras) or scramble siRNAs (Sc), and cell proteins were extracted at 24 h. *B, C*) Adult mouse cardiac fibroblasts (CFs; *B*) or MEFs (*C*) from H-*ras*$^{+/+}$ and H-*ras*$^{-/-}$ were maintained in culture. Representative immunoblots and densitometric analysis of PKG-Iβ content normalized against GAPDH are shown. *D*) MEF PKG-Iβ mRNA levels were normalized against β-actin, and the relative fold changes were determined. Values represent means ± SEM (*n* = 5). *$P < 0.05$ *vs.* H-*ras*$^{+/+}$.

increase in heart weight and ventricular size in wild-type mice (as measured by echocardiography), cardiomyocyte hypertrophy, increased TGF-β1 synthesis, and the accumulation of some ECM proteins. Any of these changes were not observed in AngII-treated H-*ras*$^{-/-}$ mice, although animal heart weights did not reach the values observed in nontreated wild-type mice, likely because of the role of other ECM proteins that have been implicated in the fibrotic process, together with the measurement techniques sensitivities used in our experiments.

The mechanisms that underlie the protective effect of H-*ras* deletion against AngII-induced cardiac damage must be considered carefully. The first mechanism that may explain the cardiac remodeling improvement that was observed in AngII-treated H-*ras*$^{-/-}$ mice is the decreased blood pressure, as a direct relationship between blood pressure and cardiac remodeling has been extensively demonstrated (35, 36). In fact, both basal and AngII-treated H-*ras*$^{-/-}$ mice exhibited decreased arterial pressures compared with their respective controls, likely because of PKG-Iβ overexpression at the vascular level (17), and these hemodynamic changes may explain the improvement in cardiac remodeling that was observed in the absence of H-*ras*. Conversely, a direct role for Ras proteins in hypertrophy, hyperplasia,

and fibrosis has also been described. There is a close relationship between the profibrotic cytokine, TGF-β1, and Ras signaling pathways (22, 39, 40). Many growth factors, in addition to Ang II, initiate intracellular signaling pathways that converge on Ras activation in cardiac fibroblasts, renal tissues, and fibroblasts and vascular smooth muscle cells (14, 41, 42). In addition, AngII activates EGF receptors *via* a transactivation event with subsequent hypertrophy and hyperplasia in vascular smooth muscle cells (13, 43). Moreover, the blockade of either the AngII receptor, AT1, or Ras prenylation decreased the early fibrotic response in an animal model of kidney obstruction (44)—an effect also observed using H-*ras*$^{-/-}$ mice (45). Taking into consideration all these data, we infer that the lack of H-Ras would also contribute to the decrease of hypertrophy and fibrosis in H-*ras*$^{-/-}$ mice.

However, additional evidence prompted us to explore alternative mechanisms that could also contribute to the protection provided by H-*ras* deletion in AngII-induced cardiac remodeling. First, we did not observe any correlation between blood pressure levels and cardiac hypertrophy or ECM deposition, which suggests that additional mechanisms could also be involved during cardiac protection. Second, H-*ras*$^{-/-}$ mice exhibited cardiac increased PKG-Iβ content, as
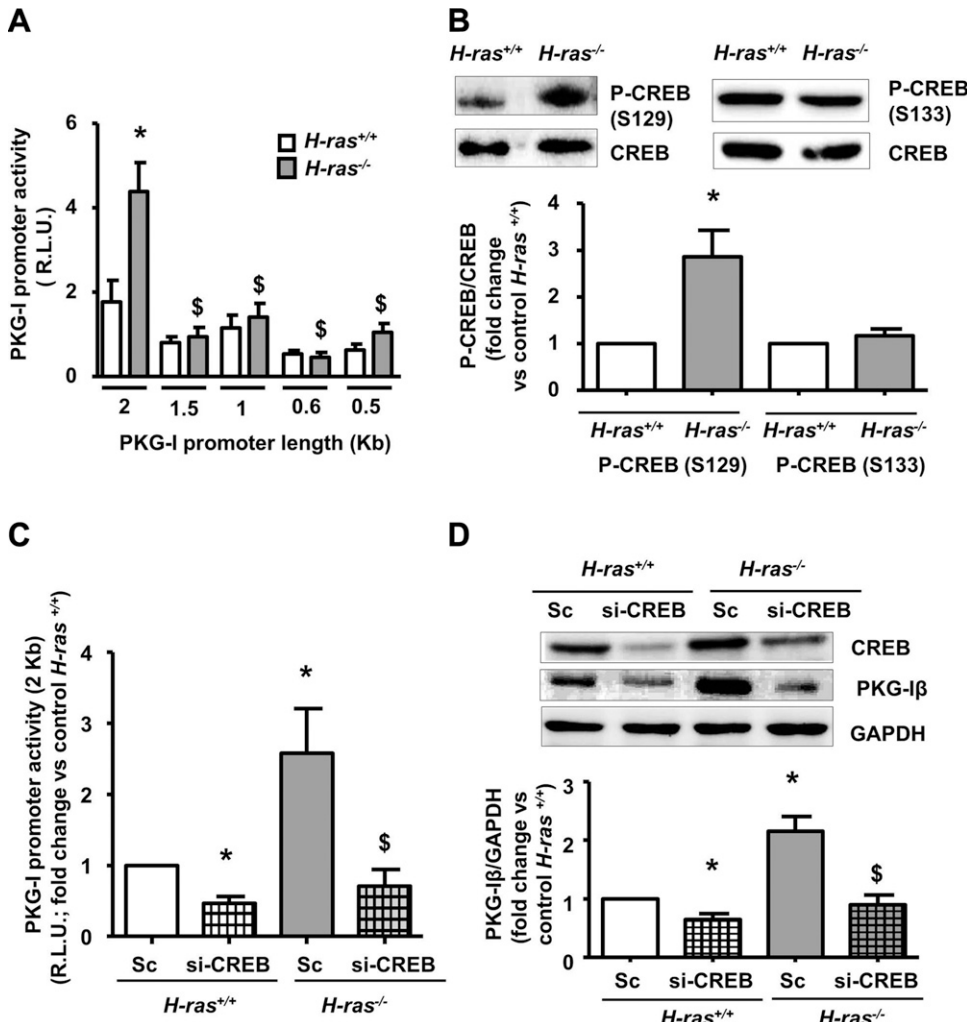
Figure 6. H-Ras deficiency increases PKG-I promoter activity and PKG-Iβ protein content *via* CREB transcriptional activity in MEFs. *A*) Cultured MEFs from H-*ras*^{+/+} and H-*ras*^{−/−} mice were transiently transfected with luciferase reporter plasmids for the PKG-I promoter region (2 kb) or with plasmids with serial deleted sections (1.5–0.5 kb), and luciferase activity (R.L.U.) was determined at 24 h. *B*) H-*ras*^{+/+} or H-*ras*^{−/−} MEF protein content was extracted. Representative immunoblots and densitometric analysis of p-CREB content at Ser129 or Ser133, normalized against total CREB content, are shown. *C*) H-*ras*^{+/+} or H-*ras*^{−/−} MEFs were transiently transfected with siRNAs against CREB (si-CREB) or scramble siRNAs as control (Sc). Twenty-four hours later, MEFs were transiently transfected with the PKG-I promoter region (2 kb) luciferase reporter plasmid, and luciferase activity was determined at 24 h. *D*) si-CREB or Sc-transfected MEF protein content was extracted 24 h after transfection. Representative immunoblots and densitometric analysis of PKG-Iβ content normalized against GAPDH are represented. Representative CREB immunoblot is shown to demonstrate successful depletion. Values represent means ± SEM ($n = 6$–10). *$P < 0.05$ *vs.* control H-*ras*^{+/+}, $P < 0.05$ *vs.* control H-*ras*^{−/−}.

already observed in vascular walls (17), with independence of AngII administration. Finally, a protective role for NO in the cardiovascular system, which prevents cardiovascular fibrosis, has also been proposed (46, 47). Thus, we hypothesized that increased PKG-Iβ that is present in H-*ras*^{−/−} hearts may constitute an
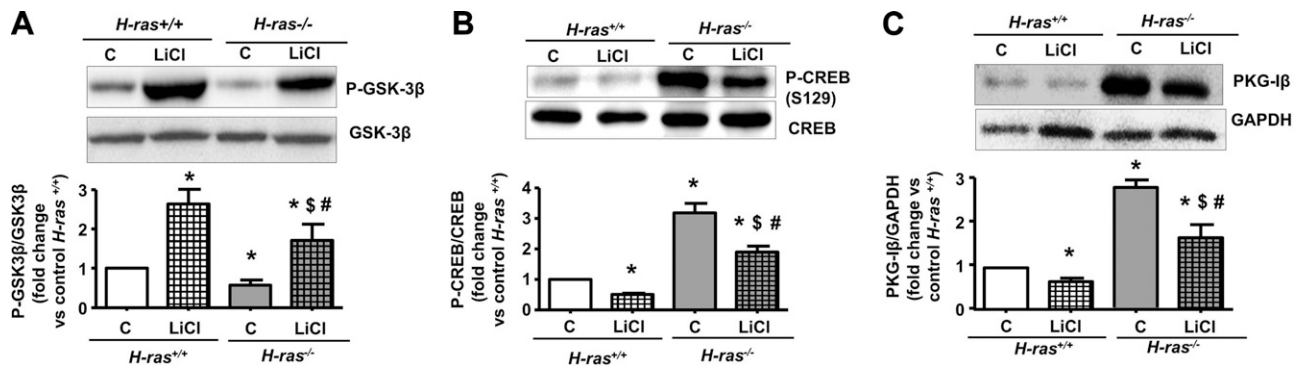

Figure 7. H-Ras deficiency increases PKG-Iβ expression and CREB activity *via* GSK-3β activation in MEFs. Cultured MEFs from H-*ras*^{+/+} and H-*ras*^{−/−} mice were treated with lithium chloride (10 mM) or vehicle (*C*) for 24 h, and protein content was extracted. Representative immunoblots and densitometric analysis of phosphorylated GSK-3β content at Ser9 normalized against total GSK-3β (*A*), phosphorylated CREB content at Ser129 (P-CREBS129) normalized against total CREB (*B*), and PKG-Iβ content normalized against GAPDH (*C*) are shown. Values represent means ± SEM ($n = 6$–10). *$P < 0.05$ *vs.* control H-*ras*^{+/+}, $P < 0.05$ *vs.* control H-*ras*^{−/−}, #$P < 0.05$ *vs.* treated H-*ras*^{+/+}.

Figure 8. H-Ras deficiency increases PKG-Iβ expression and GSK-3β–mediated CREB activation *via* the RAF/MEK/ERK pathway in MEFs. Cultured MEFs from H-*ras*$^{-/-}$ were transiently transfected with a constitutively active MEK plasmid (MEKEE) or a constitutively active mutant expression plasmid, ^{V12}RasG37, as indicated, and MEFs from H-*ras*$^{+/+}$ and H-*ras*$^{-/-}$ were transiently transfected with empty vector (*C*). Twenty-four hours after transfection, cell protein content was extracted. Representative immunoblots and densitometric analysis of p-ERK normalized against total ERK (*A*), phosphorylated GSK-3β content at Ser9 normalized against total GSK-3β (*B*), p-CREB content at Ser129 (P-CREBS129) normalized against total CREB (*C*), and PKG-Iβ content normalized against GAPDH (*D*) are shown. Values represent means ± SEM (*n* = 6–10). *$P < 0.05$ *vs.* control H-*ras*$^{+/+}$, $^{\$}P < 0.05$ *vs.* control H-*ras*$^{-/-}$.
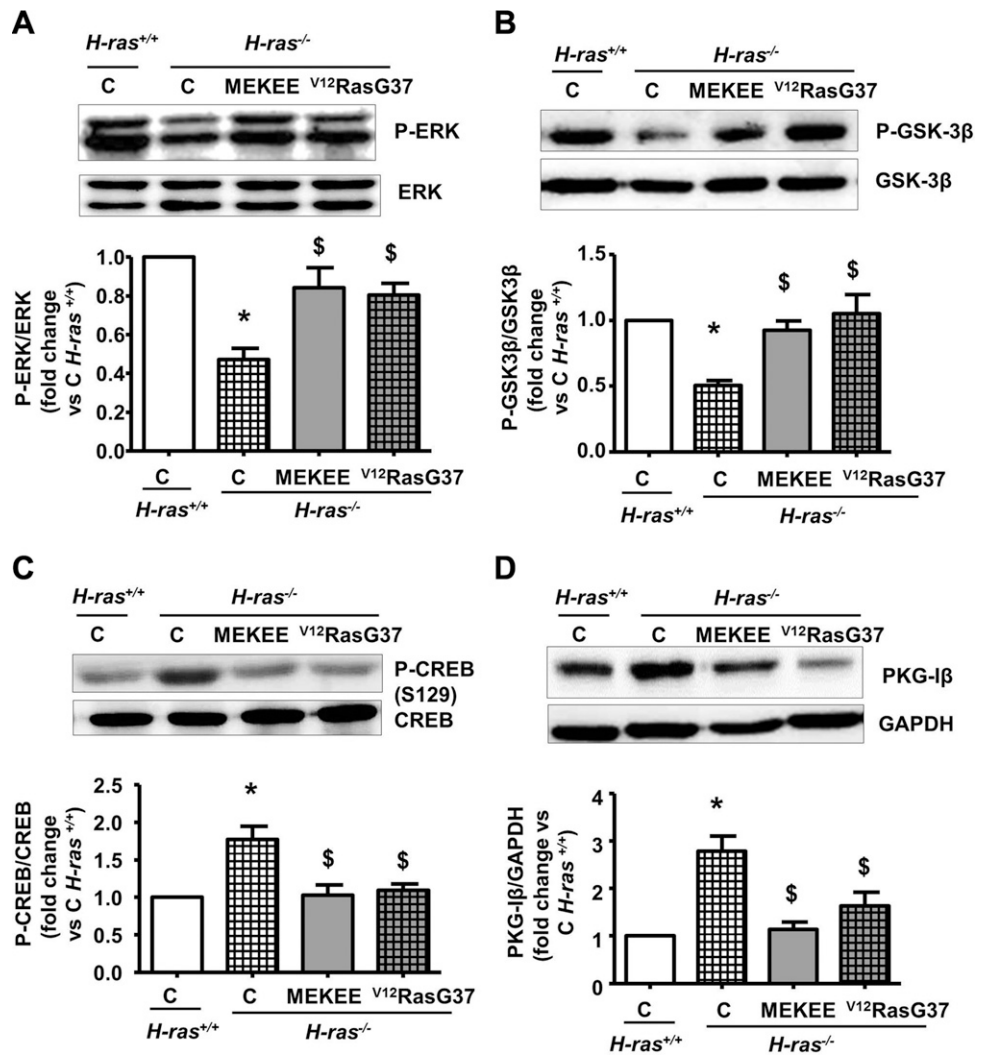
additional preventive mechanism during AngII-based cardiac remodeling.

To test this hypothesis, we considered using different experimental approaches. To exclude the influence of high blood pressure on cardiac remodeling, we discarded the strategies devoted to correct blood pressure *in vivo*, because the nonspecific effects of the selected drugs or the homeostatic responses elicited under blood pressure–lowering maneuvers could interfere in the interpretation of potential findings. Similarly, *in vivo* experiments with PKG agonists and antagonists were considered, as the exogenous modulation of the system was considered completely necessary to test our hypothesis, but were also discarded because of the complexity of analyzing the multiple potential interactions in the whole animal. Thus, we decided to perform *ex vivo* experiments in freshly dissected heart tissues from H-*ras*$^{-/-}$ and H-*ras*$^{+/+}$ mice. Basic results observed in heart explants were in agreement with those obtained in intact mice. Thus, the absence of H-Ras induced the overexpression of PKG- Iβ, and AngII significantly increased TGF-β1 and ECM protein content in heart explants from H-*ras*$^{+/+}$ animals. H-Ras deletion also prevented changes in TGF-β1 and the accumulation of matrix proteins induced by AngII in ventricular explants.

In addition, the beneficial effect of H-ras deletion on ventricular fibrosis gene marker expression disappeared by treating explants with a PKG inhibitor, and the same protective effect was elicited with the administration of PKG activators to heart explants from H-*ras*$^{+/+}$ mice. Similar results were obtained when cardiac hypertrophy gene markers were analyzed. Taken together, these results suggest that PKG-Iβ up-regulation could play a role, likely together with the hemodynamic changes, in the protective effect against AngII-induced cardiac remodeling that was observed in H-*ras*$^{-/-}$ mice hearts; however, on the basis of these explant experiments, we cannot completely assure the preventive role of PKG-Iβ overexpression in AngII-induced cardiac remodeling observed in H-Ras KO mice. Thus, additional *in vivo* experiments will be required to definitively prove this relationship.

A cardioprotective effect of the cGMP/PKG-I pathway has been reported *in vivo* and by using isolated cardiomyocytes; increased PKG-I activity protects against murine cardiac hypertrophy induced by pressure overload (48) and AngII, but not by vasoconstrictor infusion (49). Conversely, the PKG-Iβ rescue mouse line model (βRM), which expresses PKG-Iβ in smooth muscle cells and activated cardiac myofibroblasts, but not in
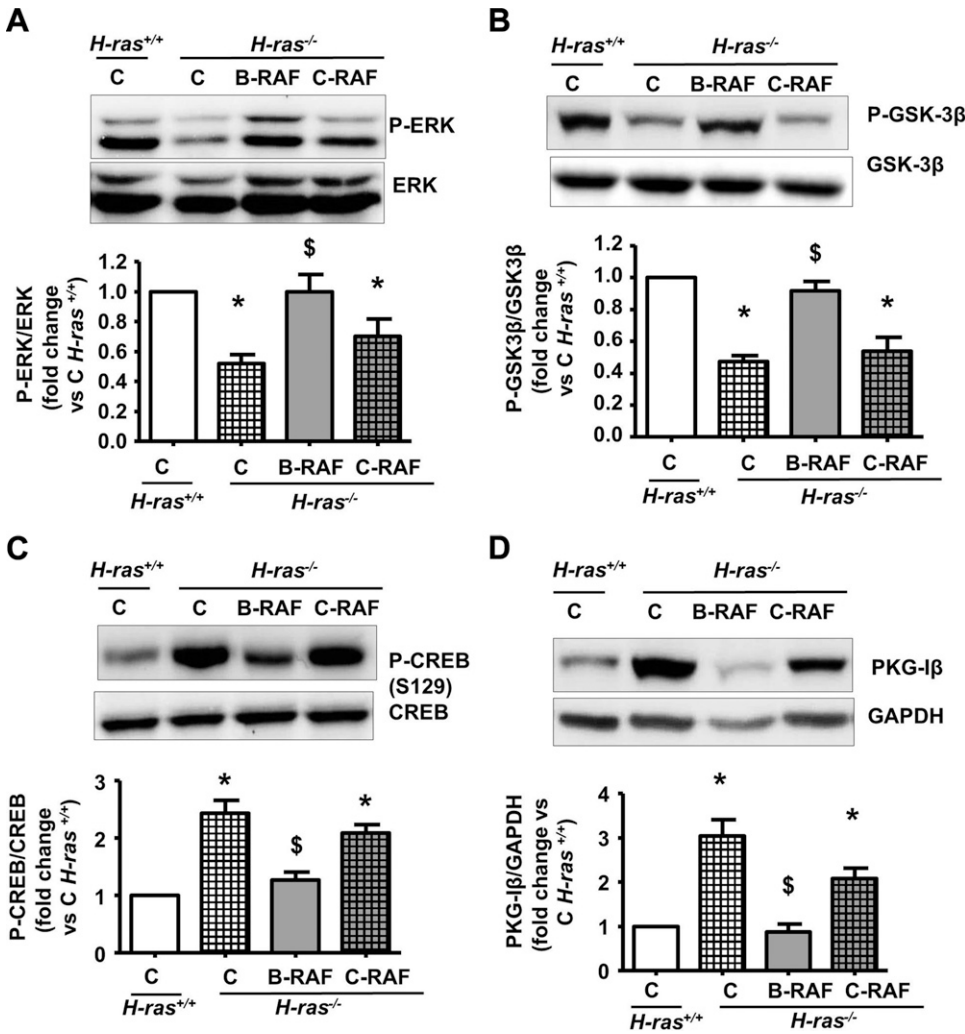
Figure 9. H-Ras deficiency increases PKG-Iβ expression and GSK-3β–mediated CREB activation *via* B-RAF in MEFs. Cultured MEFs from H-*ras*$^{-/-}$ were transiently transfected with plasmids that overexpressed B-RAF or C-RAF isoforms, and MEFs from H-*ras*$^{+/+}$ and H-*ras*$^{-/-}$ mice were transiently transfected with empty vector (*C*). Twenty-four hours after transfection, cell protein content was extracted. Representative immunoblots and densitometric analysis of p-ERK normalized against total ERK (*A*), phosphorylated GSK-3β content at Ser9 normalized against total GSK-3β (*B*), p-CREB content at Ser129 (P-CREBS129) normalized against total CREB (*C*), and PKG-Iβ content normalized against GAPDH (*D*) are shown. Values represent means ± SEM (n = 6–10). *$P < 0.05$ *vs.* control H-*ras*$^{+/+}$, $^{\$}P < 0.05$ *vs.* control H-*ras*$^{-/-}$.

cardiomyocytes, endothelial cells, or fibroblasts, developed the same degree of cardiac hypertrophy as their littermate controls when subjected to vasoconstrictor infusion, thoracic aorta constriction (50), or AngII infusion (51). Differences with some previously reported works and our results could be explained by differences in the settings of the mice models: the basal cardiomyocyte PKG-I activity was low in the animal model βRM that was used, although it may confer potent brake-like effects if sufficiently activated, as occurs in our H-*ras*$^{-/-}$ model. In fact, PKG activity—determined by p-VASP increase—seemed to be increased in H-*ras*$^{-/-}$ mice and their isolated cells compared with controls, in accordance with PKG-Iβ overexpression. In contrast, it is plausible that H-*ras* deletion affects other cGMP pathway upstream components, which may enhance the PKG activity or the antihypertrophic effect in addition to the novel signaling pathway described here. There are more conflicting results on the use of the phosphodiesterase 5 inhibitor, sildenafil, which elevates the cGMP content and increases PKG-I activity. In a mouse model with cardiomyocyte-specific overexpression of the AngII type 1 receptor, sildenafil treatment did not prevent heart hypertrophy and fibrosis (52). Sildenafil reversed thoracic aorta constriction–induced cardiac hypertrophy (48),

whereas little antihypertrophic effect in wild-type mice and no effect in βRM mice with AngII infusion was observed (51), although, in the same study, a large effect of sildenafil was observed on fibrosis in wild-type, but not βRM mice, which suggests that PKG-I present in cardiac cells is an important regulator of cardiac fibrosis (51). With regard to the differences between our data and some of the above-mentioned works, it is important to note the length of AngII treatment. An initial phase of AngII-induced cardiac hypertrophy for 7 d (51) is not comparable to a prolonged AngII treatment (28 d), such as in our model or the work from Frantz *et al.* (49) in which chronic AngII infusion (14 d) provoked dilated cardiomyopathy with a marked deterioration of cardiac function in mice with cardiomyocyte-restricted PKG-I deletion. Finally, the works mentioned above, which established that PKG has either a minor role or none in cardiac hypertrophy, refer to the Iα isoform, not to Iβ, whereas the present work studied specifically the role of PKG-Iβ.

Although the most relevant findings of the present experiments indicate that the absence of H-Ras attenuates AngII-induced cardiac remodeling and fibrosis, they also suggest that this structural improvement ameliorates the cardiac dysfunction that has been observed in chronically hypertensive mice. In fact, AngII induced left ventricular
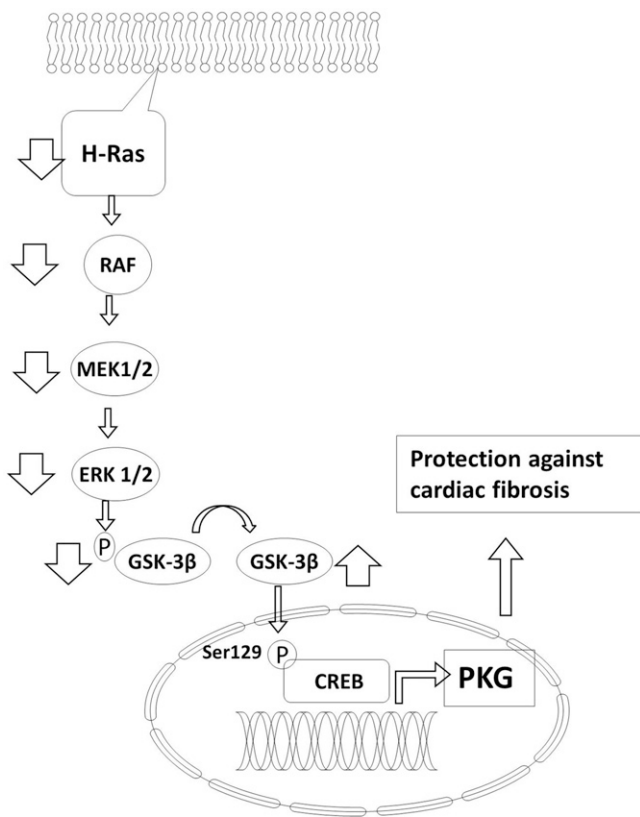
Figure 10. Proposed mechanism that links H-Ras deletion with PKG-Iβ overexpression. On the basis of the accumulated evidence, the schematic diagram illustrates the proposed intracellular pathway by which H-ras deletion results in protection against cardiac fibrosis *via* PKG-Iβ overexpression. Small arrows indicate pathway direction, large downward arrows indicate down-regulation, and large upward arrows indicate up-regulation.

dysfunction, measured as left ventricular ejection fraction and fractional shortening, in H-$ras^{+/+}$ mice, but not in H-$ras^{-/-}$ mice.

No previous reports have explained the link between H-Ras deficiency and PKG-Iβ overexpression. To try to define this relationship, we designed different experiments in cultured cells. Because a significant number of cultured cells were required, we preferred to work with MEFs that exhibited the same pattern of PKG-Iβ modulation as cardiac tissue, cardiac fibroblasts isolated from the hearts of adult animals, and a mouse cardiac muscle cell line when H-Ras was absent. We hypothesized that the canonical Ras/RAF/MEK/ERK pathway must be involved in the genesis of the observed changes, but we had no information about the possible downstream elements that link this classic cascade to the PKG promoter. By using a combined approach that included the analysis of serial promoter deletion activity, ChIP assay, the study of phosphorylation patterns in the implicated proteins, and the evaluation of PKG modulation after genetic silencing, we first determined that CREB was the transcription factor involved in PKG-Iβ up-regulation in the absence of H-Ras. Of interest, when CREB acts as PKG-Iβ regulator after H-ras deletion, it is phosphorylated

at Ser129 and not at the most frequently modulated serine residue, Ser133 (29). With regard to the possible activator of CREB when H-*ras* is absent, we selected GSK-3β, as it is inactivated when phosphorylated (30) and is able to phosphorylate CREB at Ser129 (29). Experiments with the GSK-3β inhibitor, lithium chloride, confirmed the role of this protein in CREB phosphorylation and PKG-Iβ modulation in MEFs from H-$ras^{-/-}$ animals. Finally, we established the link between H-Ras deletion, GSK-3β, and CREB with experiments, including genetic overexpression or down-regulation of the H-Ras canonical pathway downstream proteins. In addition, we demonstrated that B-RAF, and not C-RAF, was the RAF isoform that is implicated in the signaling pathway that links H-Ras and PKG-Iβ.

In summary, although hemodynamic modifications must be relevant in the genesis of cardiac changes observed in the present experiments, results suggest that overexpression of PKG-Iβ in H-$ras^{-/-}$ mice could contribute to the protection, at least in part, against AngII-induced cardiovascular remodeling (*i.e.*, cardiac hypertrophy and cardiac fibrosis). Moreover, we identified an intracellular cascade that links H-Ras deletion to PKG-Iβ overexpression (Fig. 10). Our results point to H-Ras and/or its downstream proteins as therapeutic targets and indicate that their blockade could ameliorate AngII-induced inappropriate cardiac remodeling. FJ

AUTHOR CONTRIBUTIONS

L. Calleros and D. Rodríguez-Puyol designed research; P. Martín-Sánchez, E. Lara-Pezzi, S. de Frutos, M. Rodríguez-Puyol, L. Calleros, and D. Rodríguez-Puyol analyzed data; P. Martin-Sánchez, A. Luengo, M. Griera, M. J. Orea, M. López-Olañeta, and L. Calleros performed research; S. de Frutos, M. Rodríguez-Puyol, L. Calleros, and D. Rodríguez-Puyol wrote the paper; and A. Chiloeches contributed new reagents or analytic tools.

REFERENCES

1. McKay, M. M., and Morrison, D. K. (2007) Integrating signals from RTKs to ERK/MAPK. *Oncogene* **26**, 3113–3121
2. Takai, Y., Sasaki, T., and Matozaki, T. (2001) Small GTP-binding proteins. *Physiol. Rev.* **81**, 153–208

3. Barbacid, M. (1987) Ras genes. *Annu. Rev. Biochem.* **56**, 779–827

4. Lowy, D. R., and Willumsen, B. M. (1993) Function and regulation of ras. *Annu. Rev. Biochem.* **62**, 851–891

5. Macara, I. G., Lounsbury, K. M., Richards, S. A., McKiernan, C., and Bar-Sagi, D. (1996) The *ras* superfamily of GTPases. *FASEB J.* **10**, 625–630

6. Dhanasekaran, N., and Premkumar Reddy, E. (1998) Signaling by dual specificity kinases. *Oncogene* **17**(11 Reviews), 1447–1455

7. Ehrhardt, A., David, M. D., Ehrhardt, G. R., and Schrader, J. W. (2004) Distinct mechanisms determine the patterns of differential activation of H-Ras, N-Ras, K-Ras 4B, and M-Ras by receptors for growth factors or antigen. *Mol. Cell. Biol.* **24**, 6311–6323

8. Johnson, L., Greenbaum, D., Cichowski, K., Mercer, K., Murphy, E., Schmitt, E., Bronson, R. T., Umanoff, H., Edelmann, W., Kucherlapati, R., and Jacks, T. (1997) K-ras is an essential gene in the mouse with partial functional overlap with N-ras. *Genes Dev.* **11**, 2468–2481

9. Koera, K., Nakamura, K., Nakao, K., Miyoshi, J., Toyoshima, K., Hatta, T., Otani, H., Aiba, A., and Katsuki, M. (1997) K-ras is essential for the development of the mouse embryo. *Oncogene* **15**, 1151–1159

10. Esteban, L. M., Vicario-Abejón, C., Fernández-Salguero, P., Fernández-Medarde, A., Swaminathan, N., Yienger, K., Lopez, E., Malumbres, M., McKay, R., Ward, J. M., Pellicer, A., and Santos, E. (2001) Targeted genomic disruption of H-ras and N-ras, individually or in combination, reveals the dispensability of both loci for mouse growth and development. *Mol. Cell. Biol.* **21**, 1444–1452

11. Plowman, S. J., Williamson, D. J., O'Sullivan, M. J., Doig, J., Ritchie, A. M., Harrison, D. J., Melton, D. W., Arends, M. J., Hooper, M. L., and Patek, C. E. (2003) While K-ras is essential for mouse development, expression of the K-ras 4A splice variant is dispensable. *Mol. Cell. Biol.* **23**, 9245–9250

12. Satoh, S., Rensland, H., and Pfitzer, G. (1993) Ras proteins increase Ca^{2+}-responsiveness of smooth muscle contraction. *FEBS Lett.* **324**, 211–215

13. Ohtsu, H., Suzuki, H., Nakashima, H., Dhobale, S., Frank, G. D., Motley, E. D., and Eguchi, S. (2006) Angiotensin II signal transduction through small GTP-binding proteins: mechanism and significance in vascular smooth muscle cells. *Hypertension* **48**, 534–540

14. Li, L., Fan, D., Wang, C., Wang, J. Y., Cui, X. B., Wu, D., Zhou, Y., and Wu, L. (2011) Angiotensin II increases periostin expression *via* Ras/p38 MAPK/CREB and ERK1/2/TGF-β1 pathways in cardiac fibroblasts. *Cardiovasc. Res.* **91**, 80–89

15. Brown, R. D., Ambler, S. K., Mitchell, M. D., and Long, C. S. (2005) The cardiac fibroblast: therapeutic target in myocardial remodeling and failure. *Annu. Rev. Pharmacol. Toxicol.* **45**, 657–687

16. Baker, K. M., Chernin, M. I., Wixson, S. K., and Aceto, J. F. (1990) Renin-angiotensin system involvement in pressure-overload cardiac hypertrophy in rats. *Am. J. Physiol.* **259**, H324–H332

17. Chamorro-Jorganes, A., Grande, M. T., Herranz, B., Jerkic, M., Griera, M., Gonzalez-Nuñez, M., Santos, E., Rodriguez-Puyol, D., Lopez-Novoa, J. M., and Rodriguez-Puyol, M. (2010) Targeted genomic disruption of H-ras induces hypotension through a NO-cGMP-PKG pathway-dependent mechanism. *Hypertension* **56**, 484–489

18. Potenza, N., Vecchione, C., Notte, A., De Rienzo, A., Rosica, A., Bauer, L., Affuso, A., De Felice, M., Russo, T., Poulet, R., Cifelli, G., De Vita, G., Lembo, G., and Di Lauro, R. (2005) Replacement of K-Ras with H-Ras supports normal embryonic development despite inducing cardiovascular pathology in adult mice. *EMBO Rep.* **6**, 432–437

19. Schuhmacher, A. J., Guerra, C., Sauzeau, V., Cañamero, M., Bustelo, X. R., and Barbacid, M. (2008) A mouse model for Costello syndrome reveals an Ang II-mediated hypertensive condition. *J. Clin. Invest.* **118**, 2169–2179

20. Panse, K. D., Felkin, L. E., López-Olañeta, M. M., Gómez-Salinero, J., Villalba, M., Muñoz, L., Nakamura, K., Shimano, M., Walsh, K., Barton, P. J. R., Rosenthal, N., and Lara-Pezzi, E. (2012) Follistatin-like 3 mediates paracrine fibroblast activation by cardiomyocytes. *J. Cardiovasc. Transl. Res.* **5**, 814–826

21. Martínez-Salgado, C., Fuentes-Calvo, I., García-Cenador, B., Santos, E., and López-Novoa, J. M. (2006) Involvement of H- and N-Ras isoforms in transforming growth factor-β1-induced proliferation and in collagen and fibronectin synthesis. *Exp. Cell Res.* **312**, 2093–2106

22. Chamorro-Jorganes, A., Calleros, L., Griera, M., Saura, M., Luengo, A., Rodriguez-Puyol, D., and Rodriguez-Puyol, M. (2011) Fibronectin upregulates cGMP-dependent protein kinase type Iβ through C/EBP transcription factor activation in contractile cells. *Am. J. Physiol. Cell Physiol.* **300**, C683–C691

23. Calleros, L., Sánchez-Hernández, I., Baquero, P., Toro, M. J., and Chiloeches, A. (2009) Oncogenic Ras, but not (V600E)B-RAF, protects from cholesterol depletion-induced apoptosis through the PI3K/AKT pathway in colorectal cancer cells. *Carcinogenesis* **30**, 1670–1677

24. Garnett, M. J., Rana, S., Paterson, H., Barford, D., and Marais, R. (2005) Wild-type and mutant B-RAF activate C-RAF through distinct mechanisms involving heterodimerization. *Mol. Cell* **20**, 963–969

25. Martín, P., Mora, I., Cortes, M. A., Calleros, L., García-Jerez, A., Ortiz, A., Rodríguez-Puyol, M., Rodríguez-Puyol, D., and Olmos, G. (2014) Relevant role of PKG in the progression of fibrosis induced by TNF-like weak inducer of apoptosis. *Am. J. Physiol. Renal Physiol.* **307**, F75–F85

26. Felkin, L. E., Narita, T., Germack, R., Shintani, Y., Takahashi, K., Sarathchandra, P., López-Olañeta, M. M., Gómez-Salinero, J. M., Suzuki, K., Barton, P. J., Rosenthal, N., and Lara-Pezzi, E. (2011) Calcineurin splicing variant calcineurin Aβ1 improves cardiac function after myocardial infarction without inducing hypertrophy. *Circulation* **123**, 2838–2847

27. Sugiura, T., Nakanishi, H., and Roberts, J. D., Jr. (2008) Proteolytic processing of cGMP-dependent protein kinase I mediates nuclear cGMP signaling in vascular smooth muscle cells. *Circ. Res.* **103**, 53–60

28. Ballestar, E., Paz, M. F., Valle, L., Wei, S., Fraga, M. F., Espada, J., Cigudosa, J. C., Huang, T. H., and Esteller, M. (2003) Methyl-CpG binding proteins identify novel sites of epigenetic inactivation in human cancer. *EMBO J.* **22**, 6335–6345

29. Wang, Z., Iwasaki, M., Ficara, F., Lin, C., Matheny, C., Wong, S. H., Smith, K. S., and Cleary, M. L. (2010) GSK-3 promotes conditional association of CREB and its coactivators with MEIS1 to facilitate HOX-mediated transcription and oncogenesis. *Cancer Cell* **17**, 597–608

30. Ryves, W. J., and Harwood, A. J. (2001) Lithium inhibits glycogen synthase kinase-3 by competition for magnesium. *Biochem. Biophys. Res. Commun.* **280**, 720–725

31. Ding, Q., Xia, W., Liu, J. C., Yang, J. Y., Lee, D. F., Xia, J., Bartholomeusz, G., Li, Y., Pan, Y., Li, Z., Bargou, R. C., Qin, J., Lai, C. C., Tsai, F. J., Tsai, C. H., and Hung, M. C. (2005) Erk associates with and primes GSK-3beta for its inactivation resulting in upregulation of beta-catenin. *Mol. Cell* **19**, 159–170

32. Kim, N. N., Villarreal, F. J., Printz, M. P., Lee, A. A., and Dillmann, W. H. (1995) Trophic effects of angiotensin II on neonatal rat cardiac myocytes are mediated by cardiac fibroblasts. *Am. J. Physiol.* **269**, E426–E437

33. Susic, D., Nuñez, E., Frohlich, E. D., and Prakash, O. (1996) Angiotensin II increases left ventricular mass without affecting myosin isoform mRNAs. *Hypertension* **28**, 265–268

34. Miyata, S., and Haneda, T. (1994) Hypertrophic growth of cultured neonatal rat heart cells mediated by type 1 angiotensin II receptor. *Am. J. Physiol.* **266**, H2443–H2451

35. Berk, B. C., Fujiwara, K., and Lehoux, S. (2007) ECM remodeling in hypertensive heart disease. *J. Clin. Invest.* **117**, 568–575

36. Yamamoto, K., Ohishi, M., Katsuya, T., Ito, N., Ikushima, M., Kaibe, M., Tatara, Y., Shiota, A., Sugano, S., Takeda, S., Rakugi, H., and Ogihara, T. (2006) Deletion of angiotensin-converting enzyme 2 accelerates pressure overload-induced cardiac dysfunction by increasing local angiotensin II. *Hypertension* **47**, 718–726

37. Rosenkranz, S. (2004) TGF-beta1 and angiotensin networking in cardiac remodeling. *Cardiovasc. Res.* **63**, 423–432

38. Leask, A. (2007) TGFbeta, cardiac fibroblasts, and the fibrotic response. *Cardiovasc. Res.* **74**, 207–212

39. Alcock, R. A., Dey, S., Chendil, D., Inayat, M. S., Mohiuddin, M., Hartman, G., Chatfield, L. K., Gallicchio, V. S., and Ahmed, M. M. (2002) Farnesyltransferase inhibitor (L-744,832) restores TGF-beta type II receptor expression and enhances radiation sensitivity in K-ras mutant pancreatic cancer cell line MIA PaCa-2. *Oncogene* **21**, 7883–7890

40. Park, B. J., Park, J. I., Byun, D. S., Park, J. H., and Chi, S. G. (2000) Mitogenic conversion of transforming growth factor-beta1 effect by oncogenic Ha-Ras-induced activation of the mitogen-activated protein kinase signaling pathway in human prostate cancer. *Cancer Res.* **60**, 3031–3038

41. Muthalif, M. M., Karzoun, N. A., Gaber, L., Khandekar, Z., Benter, I. F., Saeed, A. E., Parmentier, J. H., Estes, A., and Malik, K. U. (2000) Angiotensin II-induced hypertension: contribution of Ras GTPase/mitogen-activated protein kinase and cytochrome P450 metabolites. *Hypertension* **36**, 604–609

42. Schieffer, B., Paxton, W. G., Chai, Q., Marrero, M. B., and Bernstein, K. E. (1996) Angiotensin II controls p21ras activity *via* pp60c-src. *J. Biol. Chem.* **271**, 10329–10333

43. Eguchi, S., Iwasaki, H., Ueno, H., Frank, G. D., Motley, E. D., Eguchi, K., Marumo, F., Hirata, Y., and Inagami, T. (1999) Intracellular signaling of angiotensin II-induced p70 S6 kinase phosphorylation at Ser(411) in vascular smooth muscle cells. Possible requirement of epidermal growth factor receptor, Ras, extracellular signal-regulated kinase, and Akt. *J. Biol. Chem.* **274**, 36843–36851

44. Rodríguez-Peña, A. B., Fuentes-Calvo, I., Docherty, N. G., Arévalo, M., Grande, M. T., Eleno, N., Pérez-Barriocanal, F., and López-Novoa, J. M. (2014) Effect of angiotensin II and small GTPase Ras signaling pathway inhibition on early renal changes in a murine model of obstructive nephropathy. *BioMed Res. Int.* **2014**, 124902

45. Grande, M. T., Fuentes-Calvo, I., Arévalo, M., Heredia, F., Santos, E., Martínez-Salgado, C., Rodríguez-Puyol, D., Nieto, M. A., and López-Novoa, J. M. (2010) Deletion of H-Ras decreases renal fibrosis and myofibroblast activation following ureteral obstruction in mice. *Kidney Int.* **77**, 509–518

46. Goto, D., Fujii, S., Zaman, A. K., Sakuma, I., Gao, M., Koyama, T., Mitchell, J., Woodcock-Mitchell, J., Sobel, B. E., and Kitabatake, A. (1999) Long-term blockade of nitric oxide synthesis in rats modulates coronary capillary network remodeling. *Angiogenesis* **3**, 137–146

47. Kataoka, C., Egashira, K., Inoue, S., Takemoto, M., Ni, W., Koyanagi, M., Kitamoto, S., Usui, M., Kaibuchi, K., Shimokawa, H., and Takeshita, A. (2002) Important role of Rho-kinase in the pathogenesis of cardiovascular inflammation and remodeling induced by long-term blockade of nitric oxide synthesis in rats. *Hypertension* **39**, 245–250

48. Takimoto, E., Champion, H. C., Li, M., Belardi, D., Ren, S., Rodriguez, E. R., Bedja, D., Gabrielson, K. L., Wang, Y., and Kass, D. A. (2005) Chronic inhibition of cyclic GMP phosphodiesterase 5A prevents and reverses cardiac hypertrophy. *Nat. Med.* **11**, 214–222

49. Frantz, S., Klaiber, M., Baba, H. A., Oberwinkler, H., Völker, K., Gaβner, B., Bayer, B., Abeβer, M., Schuh, K., Feil, R., Hofmann, F., and Kuhn, M. (2013) Stress-dependent dilated cardiomyopathy in mice with cardiomyocyte-restricted inactivation of cyclic GMP-dependent protein kinase I. *Eur. Heart J.* **34**, 1233–1244

50. Lukowski, R., Rybalkin, S. D., Loga, F., Leiss, V., Beavo, J. A., and Hofmann, F. (2010) Cardiac hypertrophy is not amplified by deletion of cGMP-dependent protein kinase I in cardiomyocytes. *Proc. Natl. Acad. Sci. USA* **107**, 5646–5651

51. Patrucco, E., Domes, K., Sbroggió, M., Blaich, A., Schlossmann, J., Desch, M., Rybalkin, S. D., Beavo, J. A., Lukowski, R., and Hofmann, F. (2014) Roles of cGMP-dependent protein kinase I (cGKI) and PDE5 in the regulation of Ang II-induced cardiac hypertrophy and fibrosis. *Proc. Natl. Acad. Sci. USA* **111**, 12925–12929

52. Straubinger, J., Schöttle, V., Bork, N., Subramanian, H., Dünnes, S., Russwurm, M., Gawaz, M., Friebe, A., Nemer, M., Nikolaev, V. O., and Lukowski, R. (2015) Sildenafil does not prevent heart hypertrophy and fibrosis induced by cardiomyocyte angiotensin II type 1 receptor signaling. *J. Pharmacol. Exp. Ther.* **354**, 406–416